FURTHER ANALYSIS OF THE NEUTRINO INTERACTIONS IN THE CERN HEAVY LIQUID BUBBLE CHAMBER

H. Burmeister, D.C. Cundy, B. Eiben, C. Franzinetti,
J. Keren, R. Møllerud, G. Myatt, A. Orkin-Lecourtois,
M. Paty, D.H. Perkins, C.A. Ramm, K. Schultze,
H. Sletten, K. Soop, R. Stump, W. Venus and
H. Yoshiki, CERN, Geneva.
(presented by G. Myatt)

I. INTRODUCTION

The CERN 500 litre freon bubble chamber has been operated in the neutrino beam during two series of runs, one in 1963 and one in 1964. We have accumulated 459 events which are attributed to the interactions of high-energy neutrinos. At various stages in the experiment, reports have been presented at the Sienna and Dubna Conferences and in Physics Letters 12, 281, (1964). In this talk I wish to outline briefly some further analysis which has been carried out since our last report.

II. THE ELASTIC INTERACTION

In the fiducial volume of the bubble chamber we have observed 236 "non-pionic" events, containing a negative muon and one or more protons. We have long realized that a considerable proportion of these events are not examples of the elastic process:

$$\nu + n \rightarrow \mu^- + p \ .$$

The most obvious source of these "non-elastic" events is an inelastic neutrino interaction giving rise to a pion which is subsequently reabsorbed in its passage through the nucleus. In our previous report [Physics Letters 12, 281 (1964)] we have attempted to calculate the number of such events on the basis of the observed one-pion events. However, an alternative approach has been suggested by a momentum analysis of those events which have small four-momentum transfer q^2 where

$$q^2 = (\vec{p}_\nu - \vec{p}_\mu)^2 - (E_\nu - E_\mu)^2 \ .$$

The analysis concerns events with $q^2 < 0.2$ (GeV/c)^2.

All momenta are projected on to the plane defined by the muon and neutrino directions (Fig. 1). The vector sum of the momenta of all protons in an event is compared with the calculated momentum of the recoil proton from an elastic interaction on a stationary neutron. In the histograms we have classified the events according to the value of their component of momentum transverse to this recoil direction. It can be seen that the multiproton events have a decidely asymmetric distribution, whereas the single proton events lie symmetrically about the direction of the calculated recoil. This suggests that in this low-q^2 sample the single proton events are predominantly elastic, whereas the multiproton events are predominantly inelastic.

Unfortunately, this type of analysis is not feasible at high q^2 since the recoil directions in elastic and inelastic events become more similar. However, we expect that at high q^2 a certain number of true elastic events will have several protons visible as a result of nuclear interactions of the recoil, since the kinetic energy T_p of the proton is related to q^2 by the equation

$$q^2 = 2MT_p , \quad (M = \text{proton mass})$$

Therefore, a Monte-Carlo calculation has been performed to determine, as a function of q^2, the proportion of true elastic events which would have more than one proton track. The result is that the number of multiproton events which we should expect, corresponding to the observed number of single proton events, is quite small, i.e., 12%. In fact, among the non-pionic events the numbers of single-proton and multiproton events are about equal.

In order to obtain the cross-section for the elastic process and to estimate the axial vector form factor F_A we have used the following analysis. We have considered only those events with visible energy greater than 1 GeV, since at lower energy the various forms of background are higher and the q^2 distribution is not very sensitive to the form factors. We have then 120 non-pionic events of which 48 have more than one proton of kinetic energy greater than 30 MeV. (This cut-off has been applied in order not to take into account evaporation protons.) For the remaining 72 events we have calculated the quantity M^{*2} where

$$M^{*2} = (E_\nu + M - E_\mu)^2 - (\vec{p}_\nu - \vec{p}_\mu)^2 .$$

A histogram of the values of M^{*2} is shown in Fig. 2.

For true elastic events the values of M^{*2} should be distributed around the $(\text{proton mass})^2$, with smearing due to experimental errors and Fermi motion and some displacement to lower values as a result of energy loss of the recoil proton. However, it can be seen that several events have values of M^{*2} far removed from the $(\text{proton mass})^2$ and are, therefore, unlikely to be elastic. If we accept only those events with $0.48 < M^{*2} < 1.28$ $(\text{GeV})^2$, we should include all but a few percent of true elastic events. Applying this selection criterion we are left with a sample of 54 "elastic one-proton" events.

To get the total number of events we must add the expected number of elastic multiproton events, i.e., 6.5. The total elastic cross-section as a function of energy has been calculated from the numbers of events and the Van der Meer estimate of the neutrino flux (Fig. 3).

The curve is the theoretical cross-section calculated, assuming that the vector and axial vector form factors (F_A, F_V) are both equal to the electromagnetic isovector form factors. The agreement is fair; the errors shown are just statistical.

The q^2 distribution of these events (Fig. 4) has been compared with the theoretical distributions for various values of M_A in the form of F_A:

$$F_A = \frac{1}{\left(1 + \frac{q^2}{M_A^2}\right)^2}$$

The likelihood curve obtained (Fig. 5) shows a preference for M_A = 0.8 GeV, but the statistics are too poor to put a lower limit. However, we can make use of the information given by the total event rate. If we assign an uncertainty of ± 30% to the estimated flux above 1 GeV, the best fit value of M_A is 0.8 ± 0.2 GeV. For this value of M_A the "observed" number of events happens to be equal to the expected number, i.e., 60.

Thus, we can see that this analysis appears to give a fairly consistent picture of the elastic events. However, we should perhaps add two words of caution:

1) It is very difficult to determine what proportion, if any, of the selected single-proton events are not elastic.

2) The Monte-Carlo calculation is least sure at very high q^2 where there is a lack of experimental data on nucleon-nucleon scattering to serve as a check. This should not have much effect on the elastic total cross-section, but could have an appreciable effect on the form factor.

III. SINGLE PION EVENTS

In order to complement this analysis of non-pionic events we have made more detailed estimates of the absorption of pions in complex nuclei, using a Monte-Carlo calculation. If we assume that single pion production occurs mainly through the (33)-isobar, then our latest calculations indicate that absorption would take place in 50% of the cases. This would yield a number of inelastic non-pionic events comparable to the observed number of multiproton non-pionic events.

This heavy absorption makes the study of the single-pion processes very difficult in heavy nuclei. The situation is further complicated by the absorption of pions in two-pion events which can then simulate single-pion events.

IV. STRANGE PARTICLE PRODUCTION

Within the fiducial volume of the bubble chamber we have observed eight cases of strange particle production in neutrino interactions, and outside this volume a further two cases. Further study of these events has confirmed our previous statement that they are all compatible with associated production of strange particles. This statement is based on two facts:

1) The number of cases in which we see only one strange particle is compatible with our efficiency for detecting strange particle decays.

2) All the events occur above the threshold for associated production, whereas the flux of neutrinos is large below this energy.

We thought that it would be instructive to compare the relative frequency of strange particle production by neutrinos with that for other radiations. To do this we have classified our events according to the value of E′ where

$$E' = \frac{M^{*2} - M^2 - m^2}{2M} .$$

E′ is thus the lab-system energy which is required by a particle of mass m, in order to give a c.m.s. energy M^* in a collision with a stationary nucleon.

In various bands of E′ we have calculated the ratio of the number of strange particle events to the total number of inelastic events. Figure 6 shows the results of this calculation. For comparison, the curve represents the equivalent ratio for pion interactions. The statistical errors are necessarily large but the data seem to indicate that strange particles are produced at a relatively higher rate by neutrinos than they are by pions.

V. INTERMEDIATE VECTOR BOSON

As stated in our previous reports we have found no evidence for the existence of the W boson. However, we can use this lack of evidence to put lower limits on the mass M_W of the boson. In our Physics Letters paper we have stated that if the leptonic decay modes of the W predominate, $M_W > 1.8$ GeV, and if the non-leptonic modes predominate, $M_W > 1.5$ GeV. However, we can raise this latter limit somewhat if we study the distribution in momentum of the negative muon in those events which are candidates for non-leptonic W decay. In the case of elastic W production, the negative muon should have a predominantly low momentum. This is due to a simple kinematical effect. If we integrate over the neutrino spectrum above 4 GeV (where W production is most likely to dominate), we find that in over 70% of the cases of elastic W production the negative muon should have momentum < 2 GeV/c. This means that in this region we should expect 14 events if $M_W = 1.5$ GeV, and 3 events if $M_W = 1.9$ GeV.

In fact, we have observed five events which satisfy these criteria and are compatible with the non-leptonic decay of a boson with mass in the range 1.5 to 2.0 GeV. A statistical analysis of the energy distribution of these events, compared with that expected for elastic boson production, allows us to conclude with 99% confidence that $M_W > 1.7$ GeV if the non-leptonic decay modes predominate.

FIGURE CAPTIONS

Figure 1 : Low q^2 events.

Figure 2 : M^{*2} distribution of "one-proton" events.

Figure 3 : Elastic cross-section.

Figure 4 : q^2 distribution of selected "one-proton" non-pionic events $E_{vis} > 1$ GeV.

Figure 5 : Likelihood curve of fits to q^2 distribution.

Figure 6 : Ratio of strange particle events to total inelastic.

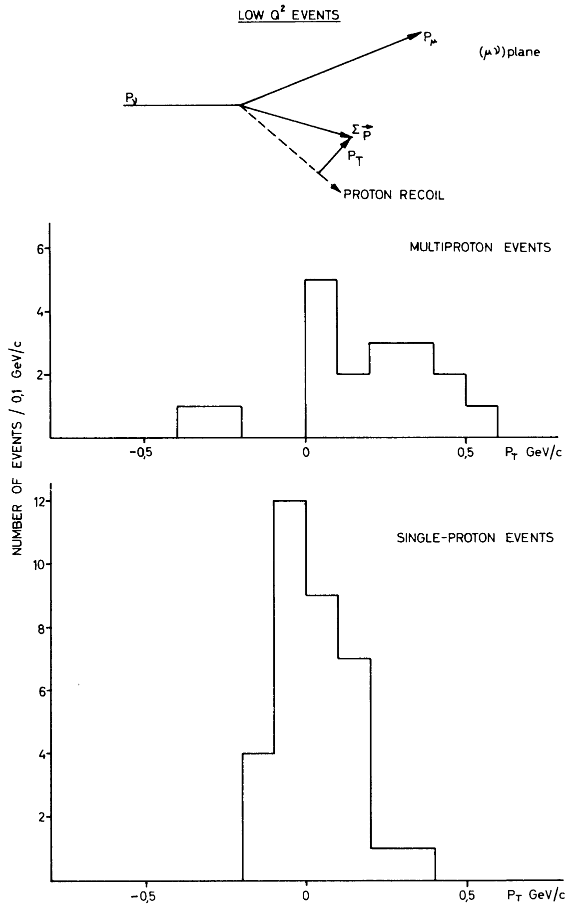
LOW Q² EVENTS
P_μ
($\mu\nu$) plane
P_ν
$\Sigma\vec{P}$
P_T
PROTON RECOIL
MULTIPROTON EVENTS
SINGLE-PROTON EVENTS
NUMBER OF EVENTS / 0,1 GeV/c
P_T GeV/c

Fig. 1

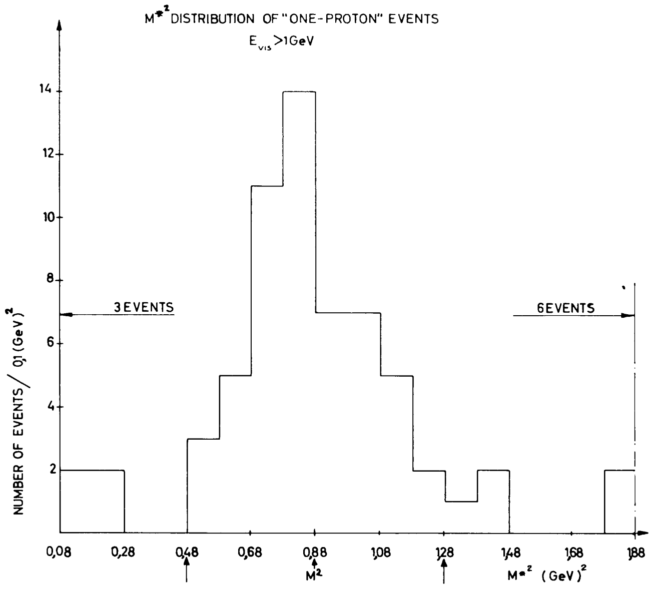
M^{*2} DISTRIBUTION OF "ONE-PROTON" EVENTS
E_{vis} > 1 GeV
3 EVENTS
6 EVENTS
NUMBER OF EVENTS / 0,1 (GeV)²
M^2
M^{*2} (GeV)²

Fig. 2

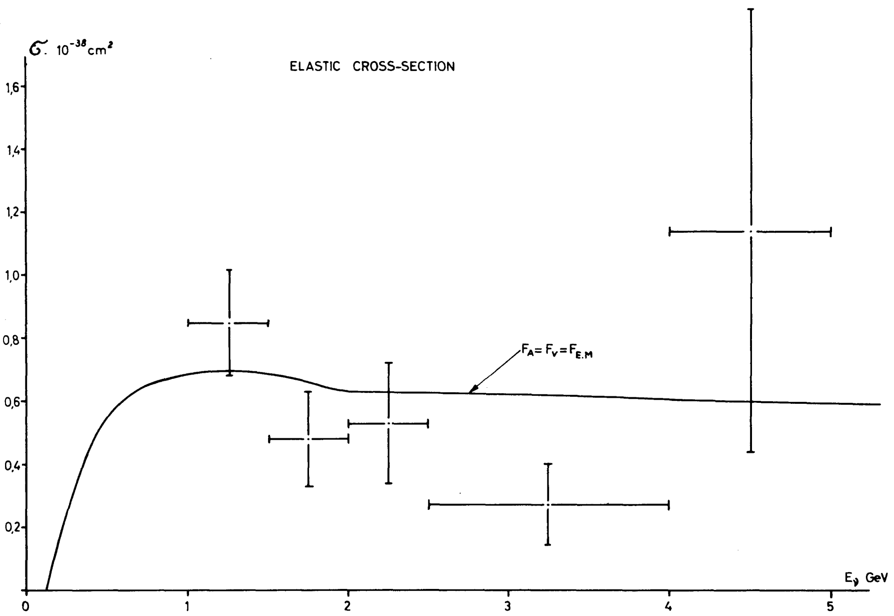

σ. 10^{-38} cm²
ELASTIC CROSS-SECTION
1,6
1,4
1,2
1,0
0,8
0,6
0,4
0,2
$F_A = F_V = F_{E.M}$
0
1
2
3
4
5
E_ν GeV

Fig. 3

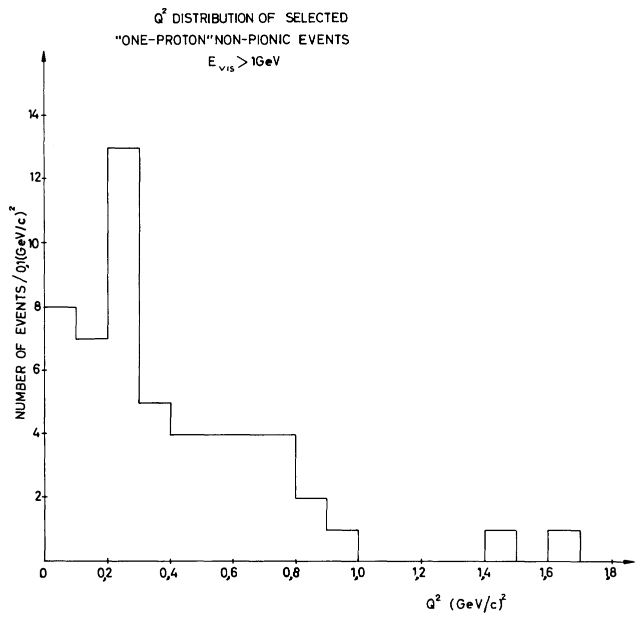

Q^2 DISTRIBUTION OF SELECTED
"ONE-PROTON" NON-PIONIC EVENTS
$E_{vis} > 1$ GeV
NUMBER OF EVENTS / 0,1 $(GeV/c)^2$
14
12
10
8
6
4
2
0
0,2
0,4
0,6
0,8
1,0
1,2
1,4
1,6
1,8
Q^2 $(GeV/c)^2$

Fig. 4

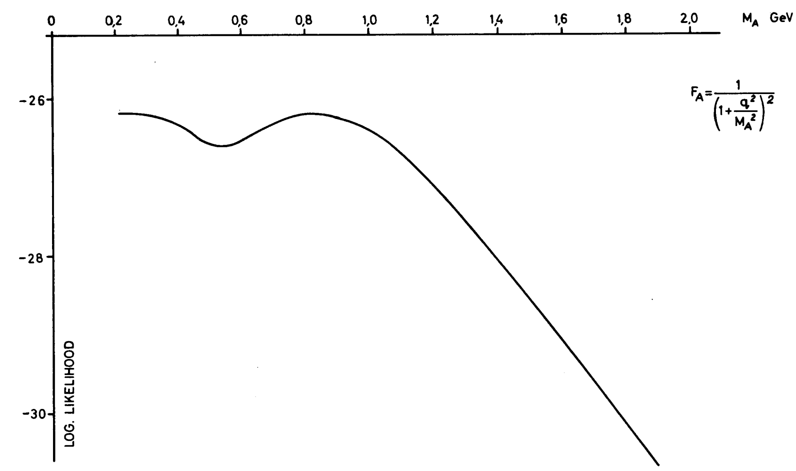

0
0,2
0,4
0,6
0,8
1,0
1,2
1,4
1,6
1,8
2,0
M_A GeV
-26
-28
-30
LOG. LIKELIHOOD
$F_A = \frac{1}{\left(1+\frac{q^2}{M_A^2}\right)^2}$

Fig. 5

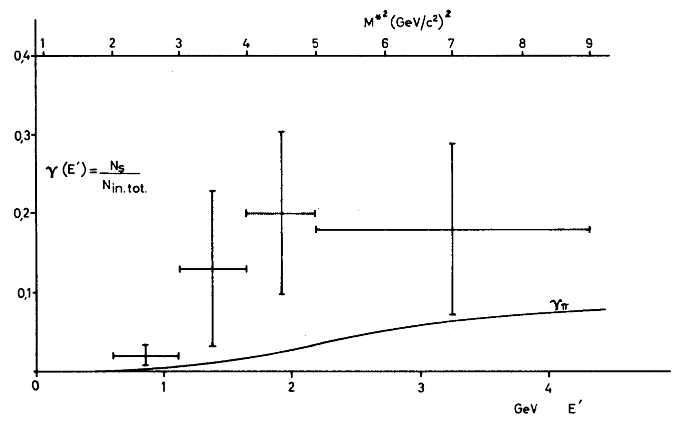

M^{*2} $(GeV/c^2)^2$
1
2
3
4
5
6
7
8
9
0,4
0,3
0,2
0,1
$\gamma(E') = \frac{N_S}{N_{in.tot.}}$
γ_π
0
1
2
3
4
GeV E′

Fig. 6